Experimental Transmission of Kaposi's Sarcoma–associated Herpesvirus (KSHV/HHV-8) to SCID-hu Thy/Liv Mice

By D. Dittmer,[‡§] C. Stoddart,[*‖] R. Renne,[‡§] V. Linquist-Stepps,[*‖] M.E. Moreno,[*‖] C. Bare,[*‖] J.M. McCune,[*‖] and D. Ganem[‡§]

*From the *Departments of Microbiology and Medicine, ‡Department of Microbiology and Immunology and Department of Medicine, and §Howard Hughes Medical Institute, University of California, San Francisco, California 94143; and ‖Gladstone Institute of Virology and Immunology, San Francisco, California 94110*

Summary

Kaposi's sarcoma–associated herpesvirus (KSHV/HHV-8) is a novel human lymphotropic herpesvirus linked to several human neoplasms. To date, no animal model for infection by this virus has been described. We have examined the susceptibility of C.B-17 *scid/scid* mice implanted with human fetal thymus and liver grafts (SCID-hu Thy/Liv mice) to KSHV infection. KSHV virions were inoculated directly into the implants, and viral DNA and mRNA production was assayed using real-time quantitative polymerase chain reaction. This revealed a biphasic infection, with an early phase of lytic replication accompanied and followed by sustained latency. Ultraviolet irradiation of the inoculum abolished all DNA- and mRNA-derived signals, and infection was inhibited by ganciclovir. Viral gene expression was most abundant in $CD19^+$ B lymphocytes, suggesting that this model faithfully mimics the natural tropism of this virus. Short-term coinfection with HIV-1 did not alter the course of KSHV replication, nor did KSHV alter levels of HIV-1 p24 during the acute phase of the infection. Although no disease was evident in infected animals, SCID-hu Thy/Liv mice should allow the detailed study of KSHV tropism, latency, and drug susceptibility.

Key words: Kaposi's sarcoma–associated herpesvirus • KSHV • SCID-hu • transmission • real-time PCR

Kaposi's sarcoma–associated herpesvirus (KSHV),[1] also called human herpesvirus (HHV)-8, is a novel member of the lymphotropic human herpesvirus family. KSHV sequences were identified initially in Kaposi's sarcoma (KS) lesions of AIDS patients (1). The virus has also been detected in a variety of AIDS-associated lymphoproliferative disorders, namely body cavity or primary effusion lymphoma (PEL; reference 2) and multicentric Castleman's disease (3). KS itself is a hyperproliferation of poorly differentiated endothelial cells and is associated with extreme neovascularization. To date, a wealth of epidemiological evidence points to a central role for KSHV in the development of KS (for review see references 4–7). For instance, KSHV DNA (8) and seroreactivity (9) directed against latent or lytic antigens can be detected in virtually all cases of KS. Seropositivity for KSHV precedes disease and is a major independent risk factor for KS in AIDS patients (10–14). Viral DNA can also be isolated from KS lesions of HIV-1–sero-negative patients (8), suggesting that KSHV is the principal viral factor involved in all epidemiological forms of this disease.

Like all herpesviruses, KSHV has two modes of infection: lytic replication, which generates infectious progeny and destroys the host cell, and latent replication, in which the viral genome persists in its host cell but with dramatically restricted gene expression and without cell destruction (15). Transcripts of latent viral genes (e.g., K12/kaposin, orf73/LANA, orf72/v-cyclin) are found in most KS tumor cells (16–19), and a subset of these transcripts (e.g., kaposin and v-cyclin) may confer a cell-autonomous proliferative advantage to the cells expressing them (20, 21). By contrast, $<3\%$ of infected cells in KS lesions or in $KSHV^+$ lymphomas display evidence of lytic KSHV gene expression (16, 22, 23). Certain lytic genes (K1, vGCR, vIRF) also transform cultures of NIH3T3 cells (24–26); however, the relevance of these observations to tumorigenesis in vivo remains to be established.

A major impediment to the study of KSHV biology has been the absence of a suitable animal or culture model for de novo infection. PEL cell lines harbor latent KSHV genomes and can be induced to produce virions by treatment

[1]*Abbreviations used in this paper:* HHV, human herpesvirus; KSHV, Kaposi's sarcoma–associated herpesvirus; PEL, primary effusion lymphoma; RT, reverse transcriptase.

 J. Exp. Med. © The Rockefeller University Press • 0022-1007/99/12/1857/12 $5.00
Volume 190, Number 12, December 20, 1999 1857–1868
http://www.jem.org

with phorbol-12-myristate-13-acetate (TPA) or sodium butyrate (22). However, most established cell lines or primary explants support only limited replication or maintenance of KSHV (27, 28). Unlike its cousin, Epstein-Barr virus (29), KSHV could not be propagated in SCID mice reconstituted with human peripheral blood cells (30), and transmission of KSHV to other conventional laboratory animals has not been reported. This suggests that the cell type most susceptible to KSHV replication and latency might be highly specialized or not readily propagated ex vivo. To alleviate the problem of inadequate in vitro systems to study natural infection, we decided to test whether KSHV could infect cells in human Thy/Liv organs grafted onto SCID mice.

The SCID-hu Thy/Liv mouse model uses C.B-17 *scid/scid* mice as recipients of human fetal liver and fetal thymus implants. Upon coimplantation of both tissues under the murine kidney capsule, human hematopoietic and lymphoid precursor cells reconstitute an organ that faithfully reproduces human multilineage hematopoiesis, including thymopoiesis (31, 32). T lymphocytes in various stages of development comprise the bulk (>90%) of cells in the implant, but cells of all hematopoietic lineages (including monocytes and B cells) and stromal endothelial cells are present. After direct injection of virus into the implant, replication of a number of human viruses is observed in the lymphoid (e.g., HIV-1 [33], HTLV-1 [34], HHV-6 [35], and varicella-zoster virus [36]) and stromal (e.g., HIV-1 [37], CMV [38], and measles virus [39]) compartments of the graft. Depending on the biology of the particular virus, the resulting infection may be noncytopathic, (e.g., CMV [38]) or may induce severe target cell depletion (e.g., HIV-1 [40] and HHV-6 [35]).

This paper shows that KSHV derived from cultured PEL cells can initiate a productive infection in SCID-hu Thy/Liv mice. Accumulation of viral DNA depends on intact virions and can be inhibited by ganciclovir. Latent and lytic transcripts can be detected principally in $CD19^+$ lymphocytes, but the morphology of the implant remains intact and no cytopathic effects are seen during acute infection. SCID-hu Thy/Liv mice represent the first animal model in which KSHV replication and persistence can be observed.

Materials and Methods

Virus Growth. BCBL-1 cells at a concentration of 5×10^5 cells/ml were induced with 20 ng/ml TPA (Calbiochem) for 12 h, reseeded in fresh medium (RPMI 1640, 10% FCS, penicillin and streptomycin, l-glutamine, sodium bicarbonate, and β-ME; all from GIBCO BRL), and cultured for an additional 4 d in 5% CO_2 at 37°C. This induction protocol results in $\sim 10^6$ DNA genome equivalents per milliliter of culture (22). Debris was removed by centrifugation for 10 min at 5,000 rpm in a GS4 rotor, and virus was pelleted by centrifugation for 2 h at 14,000 rpm in a SS-38 rotor. Virus from 180 ml supernatant was pelleted, and the pellet was resuspended in 1,000 μl PBS, of which 50 μl was injected per implant. HIV-1 NL4-3 was prepared as previously described (41).

KSHV Infection of SCID-hu Thy/Liv Mice. SCID-hu Thy/Liv mice were generated by coimplantation of fragments of human second trimester fetal liver and thymus under the kidney capsule of male homozygous C.B-17 *scid/scid* (SCID) mice (31). Implants were infected 4–7 mo after implantation by direct inoculation as previously described (42). In brief, mice were anesthetized, the left kidney was surgically exposed, and the implant was inoculated with 50 μl of virus stock. The abdominal wall incision was sutured, and the skin was closed with staples. Where indicated, ganciclovir sodium salt (Cytovene; Hoffman-La Roche) was administered intraperitoneally twice daily at 50 mg/kg/d from the day of virus inoculation. At indicated times after inoculation, mice were killed and their implants surgically removed and processed for PCR. For flow cytometry, cell sorting, and quantitative PCR, single-cell suspensions were obtained by grinding the implants between glass plates. The cells were counted in a Coulter counter and divided in aliquots for the different assays.

PCR and Reverse Transcriptase–PCR. Qualitative reverse transcriptase (RT)-PCR and subsequent Southern hybridization for lytic messages was performed as described by Renne et al. (27). Qualitative RT-PCR was performed using the same procedure with plasmid pDD4 (17) as hybridization probe. A description of the primers used in these experiments is shown in Table I. In brief, RNA was isolated using RNAzol (Tel-Test, Inc.) according to the supplier's protocol. 500 ng total RNA was reverse transcribed using 200 U of Mo-MuLV RT (GIBCO BRL) in a total volume of 20 μl containing 125 μM dATP, dGTP, and dTTP, 20 U RNasin (Promega Corp.), and 120 pmol random hexanucleotide primers (Boehringer Mannheim). After incubation at 42°C for 35 min, and the reaction was stopped by heating to 95°C for 5 min, and then 80 μl of a PCR mix containing 10× PCR Mg-Buffer (Perkin-Elmer Corp.), 100 pmol of each primer, and 5 U of Taq polymerase (Perkin-Elmer Corp.) was added and amplified over 30 cycles (30 s at 94°C, 1 min at 58°C, and 1 min 30 s at 72°C).

Quantitative DNA and RT-PCR was carried out in duplicate using Taqman® RT and Taqman® PCR with Amplitaq Gold® reagents (PE Biosystems). Reverse transcription was carried out using 2.5 μM random hexamers at 25°C for 10 min, 48°C for 30 min, and 95°C for 5 min. PCR was carried out using universal cycle conditions (2 min at 50°C, 10 min at 95°C, and then 40 cycles of 15 s at 95°C and 1 min at 60°C) on an ABI PRIZM 7000™ sequence detector (43). To prevent contamination, all PCR reactions were assembled in the segregated space in which neither KSHV virions nor cloned KSHV DNA was handled. Carryover of the amplification product was avoided using positive displacement pipettes and UNG glycosylase in the amplification reaction (44). To determine the sensitivity of the assay, RNA derived from BCBL-1 cells was used (data not shown). Quantitative analysis revealed that the signal for the lytic orf29 message was on average 50–100-fold lower than the signal for spliced latent messages in latently infected BCBL-1 cells, consistent with prior observations (22) that only 1–5% of BCBL-1 cells undergo spontaneous KSHV replication at any given time. The assay was linearly dependent on input cell number in the range of 1–10^5 infected cells per reaction). We found that KSHV could be most sensitively detected using primers that detect both spliced and nonspliced latent transcripts (primers lat-273F, lat-335R, and lat-294T; see Table I). With such primers, we were consistently able to detect 1 infected cell in 10^5 uninfected cells.

Cell Sorting and Flow Cytometry. Single-cell suspensions were incubated with biotinylated mAbs directed against human CD4, CD8, and CD3–biotin (all from Becton Dickinson) for 0.5 h in PBS and 2% FBS on ice and depleted using Dynabeads (Dynal Inc.) according to recommendations from the manufacturer. Pre- and postdepletion cell populations were stained with streptavidin–FITC and PE-conjugated mAbs directed against human CD19

(Becton Dickinson) and separated on a FACSVantage™ (Becton Dickinson) cell sorter to isolate $CD19^+$ B cells, $CD4^+$, $CD8^+$, and $CD3^+$ T cells, and cells negative for all four markers. Sort-purified cells were frozen as pellets and stored at −80°C before processing.

Results

Replication of KSHV in Human Thy/Liv Implants. To test whether KSHV would replicate in the human Thy/Liv implants of SCID-hu mice, we prepared concentrated KSHV virions from induced BCBL-1 cell supernatant (22) and inoculated 50 μl of virus suspension (containing $\sim 10^7$ genome equivalents) directly into each implant, according to established procedures (32). As an average implant contains $\sim 10^8$ human cells, the maximal multiplicity of infection is an estimated 0.1 genome equivalents per cell. However, it is likely that this substantially overestimates the true multiplicity of infection, because it is unlikely that all of the input virions are infectious (in many viruses, the particle/pfu ratio can be as high as 10^2–10^4). Each cohort included animals injected with UV-inactivated KSHV to serve as negative control; UV irradiation should completely abolish infectivity by cross-linking the double-stranded DNA genome (45–47). At various times after inoculation, the mice were killed. To have all cell types represented, the implants were removed in toto, and 2.5 μg of total implant DNA (corresponding to $\sim 4.5 \times 10^5$ cells) was assayed for the presence of viral DNA by quantitative real-time DNA PCR using

Table I. *Primers Used for Detection of Latent and Lytic Transcripts*

Latent RT-PCR		
#7209	(23mer)	5′-GCATATGCGAAGTAAGAGATTGT
#7307	(21mer)	5′-AGCAGCAGCTTGGTCCGGCTG
#7322	(24mer)	5′-GGTCCTGGGGACTCTCCACAGGAA
#7324	(25mer)	5′-AGCAGCTTGGTCCGGCTGACTTATA
orf29 RT-PCR		
#290A	(19mer)	5′-GCAGCTAGCCAACTCCGTG
#290B	(19mer)	5′-GCAGGAAACTCGTGGAGCG
GAPDH control		
gapdh-a	(24mer)	5′-CCACCCATGGCAAATTCCATGGCA
gapdh-s	(24mer)	5′-TCTAGACGGCAGGTCAGGTCCACC
Real-time quantitative RT-PCR for spliced lytic orf29		
tac29-5F	(16mer)	5′-CCCGGAGGACGGTCCA
tac29-68R	(21mer)	5′-CCCCGAATGCTCTGTTCTTATT
tac29-22T	(23mer)	5′-Fam-CTCGCTGATGTGCGCAACATGCT-Tamra
Real-time quantitative RT-PCR for unspliced latent orf73		
lat-273F	(20mer)	5′-ACTGAACACACGGACAACGG
lat-335R	(19mer)	5′-CAGGTTCTCCCATCGACGA
lat-294T	(22mer)	5′-Fam-TAGCGTACTCTCGCGGCCCAGC-Tamra
Real-time quantitative RT-PCR for spliced latent orf72		
lat-335R	(19mer)	5′-CAGGTTCTCCCATCGACGA
TAQ-F1	(21mer)	5′-AGGCAGCTGCGCCACGAAGCA
lat-294T	(22mer)	5′-Fam-TAGCGTACTCTCGCGGCCCAGC-Tamra
Ribosomal RNA		
riboF	(20mer)	5′-CGGCTACCACATCCAAGGAA
riboR	(18mer)	5′-GCTGGAATTACCGCGGCT
riboP	(22mer)	5′-Joe-TGCTGGCACCAGACTTGCCCTC-Tamra
myc		
c-mycF	(20mer)	5′-TCAAGAGGTGCCACGTCTCC
c-mycR	(22mer)	5′-TCTTGGCAGCAGGATAGTCCTT
c-mycP	(23mer)	5′-Fam-CAGCACAACTACGCAGCGCCTCC-Tamra

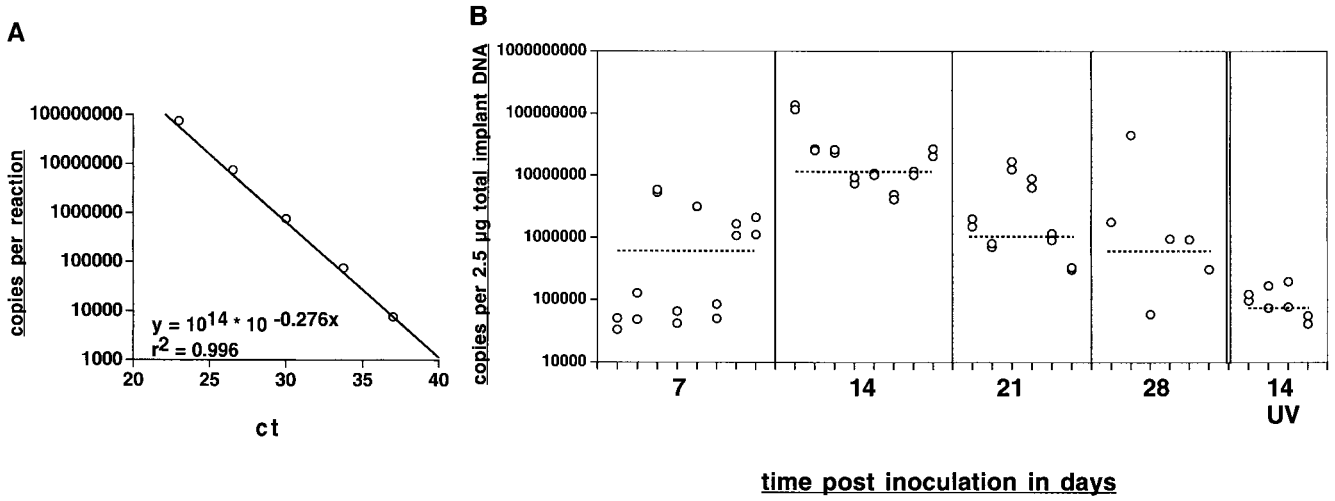

Figure 1. (A) Standard curve for quantitation of DNA copy number. The vertical axis shows copies of target DNA per reaction. The horizontal axis shows the ct values as determined by real-time quantitative PCR. (B) Time course of infection. Implants are measured in duplicates (except at day 28). Each mark (○) shows the copy number (logarithmic scale) per 2.5 μg of total implant DNA. The horizontal axis shows times after inoculation. The column labeled UV presents the signal obtained from implants that received UV-inactivated virus. The median of each group is indicated by the dashed line.

primers lat-273F, lat-335R, and lat-294T (Table I). Fig. 1 A shows a standard curve for the real-time quantitative DNA PCR to demonstrate the linear range of the assay, and Fig. 1 B shows a time course of infection. KSHV-specific DNA was low or undetectable in most implants 7 d after inoculation, peaked with a mean signal of ~100 times background at day 14, and then receded to lower levels at days 21 and 28. This increase in KSHV genome copy number between days 7 and 14 after inoculation and subsequent reduction provides evidence for initial viral replication in the implant, as would be expected in a de novo infection. Exposure of KSHV virions to UV irradiation blocked infectivity.

Assuming that, as in cultured PEL cell lines, infected cells harbor ~50 copies of episomal KSHV DNA per cell, we estimate that this level of viral DNA would correspond to infection of ~1 cell in 1,000 in the implant (see Fig. 7). As $CD19^+$ B cells represent between 0.2 and 2% of the total number of cells in the implant (31), the actual density of infection in this permissive subpopulation is likely to be higher. No difference in the levels of KSHV-specific DNA or transcripts was found between implants derived from different fetal sources ($n = 4$), indicating that susceptibility to KSHV infection is independent of the donor background.

RT-PCR for KSHV mRNAs Allows the Identification of Latent and Lytic Infection. Lytic herpesvirus replication proceeds in a regulated cascade of differential gene expression. Late lytic gene transcription in particular is dependent on viral replication and an array of viral transacting factors, whereas latent gene transcription occurs in the absence of lytic viral transactivators. If the initial increase in viral DNA noted in the SCID-hu Thy/Liv implants was indeed due to bona fide lytic replication, it should have been accompanied by late lytic gene transcription. Therefore, evidence for mRNA from orf29, a well characterized late viral gene product whose production occurs only in cells undergoing viral replication, was sought by RT-PCR. Following our previously established protocol (27), total implant RNA was isolated, reverse transcribed using random hexamers, and amplified using primers specific for lytic messages (primers 290A and 290B; Table I). Amplified products were separated on a 2% agarose gel and hybridized with ^{32}P-labeled probes specific for either product. In this assay, a cutoff was established, and only implants yielding detectable amplification products were scored positive. Primers for the amplification of the lytic orf29 message were located on opposite sides of intron #1; hence, amplification products of the proper size can derive only from late messages and not from contaminating viral DNA.

We also developed similar qualitative techniques to detect evidence for latent transcription (Fig. 2), using primers specific for either the latent nonspliced orf73 message or spliced orf72 message (primers #7209, #7307, and #7324; Table I). As for orf29, correct amplification products using orf72-specific primers can only derive from properly processed mRNA. Amplification products with orf73 primers could derive from either DNA or RNA; however, we estimate that >90% of the signal is derived from amplification of mRNA. Fig. 2 shows the location of the primers and the result of a control amplification from BCBL-1 RNA. Lanes 7–9 show evidence of latent message as judged by the presence of amplification products of the expected size (Fig. 2 B). Using primers specific for spliced orf72 message, no signal was generated in the absence of RT (compare lanes 7 and 8 to 4 and 5). Using primers for unspliced orf73 message, a faint band was detected in the absence of RT, presumably resulting from residual viral DNA (lane 6), but was strongly augmented in the presence of RT (lane 9).

Using the RT-PCR assays outlined above, evidence for productive KSHV infection could be detected in human Thy/Liv implants injected with KSHV (Table II). At day 14 after inoculation, KSHV-latent transcripts were detectable in all infected implants but not in any of the implants

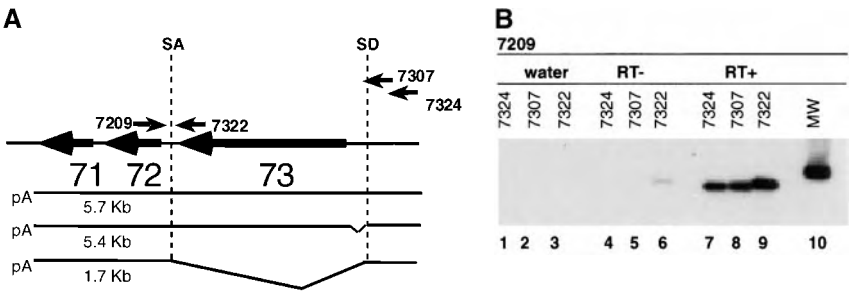

Figure 2. Primer design and control reaction for the detection of latent messages. (A) The schematic outlines the genomic organization and message structure as determined previously (17). Arrows indicate a given primer identified by its number. SD and SA denote the splice donor and splice acceptor sites, respectively. 71, 72, and 73 refer to the latent orfs of KSHV. (B) The autoradiograph of a Southern hybridization of an RT-PCR reaction using forward primer #7209 and the different primers indicated directly above each lane, which were then hybridized with a latency-specific probe. The reactions used BCBL-1–derived RNA in either the absence (RT−) or presence (RT+) of RT or with no template (water). MW, 100-bp molecular mass markers with the hybridized marker.

that were injected with UV-inactivated KSHV ($P \leq 0.005$ by X^2). Human GAPDH (glyceraldehyde-3-phosphate-dehydrogenase)-specific message could be amplified in each case. This demonstrates that infection was dependent on intact, functional virions. Up to 50% of implants harbored levels of lytic transcripts above the cutoff detectable in this assay ($P \leq 0.1$ by X^2), suggesting that lytic KSHV replication was supported in these instances (summarized in Table II). To demonstrate that these results were not specific to the BCBL-1 isolate of KSHV, the experiments were repeated with KSHV purified from the equivalent number of induced BC-3 cells (data not shown). As in previous experiments, KSHV latency–specific messages could be amplified from all implants injected with BC-3–derived KSHV but not from those injected with UV-inactivated virus. These results establish that both PEL-derived isolates are functional in this assay.

We next determined the time course of latent and lytic gene transcription. Latent transcripts were detectable in almost all animals (seven to eight of eight) up to 4 wk after inoculation and in two of four animals 16 wk after inoculation. Moreover, one of two infected mice showed evidence of latent transcripts 6 mo after inoculation. However, the fraction of implants with detectable lytic transcripts peaked at day 14 and then declined (Fig. 3). The peak of lytic gene transcription coincided with the peak of viral DNA load (as reported in Fig. 1), supporting the hypothesis that the increase in genome copy number resulted from authentic viral replication. Furthermore, no lytic transcripts were detected 21 d after inoculation, suggesting that productive infection was dramatically diminished or had ceased by that time. As before, UV inactivation of the virus abolished both latent and lytic signals.

Table II. *KSHV Transcript Analysis of Infected Implants*

Experiment	Time	Virus	RT-PCR gapdh	RT-PCR Latent	RT-PCR Lytic
	d				
1	14	BCBL-1	7/7	7/7	2/7
	14	BCBL-1 and UV	3/3	0/3	0/3
				$P \leq 0.005$	$P \leq 0.3$
2	14	BCBL-1	8/8	8/8	4/8
	14	BCBL-1 and UV	3/3	0/4	0/4
				$P \leq 0.005$	$P \leq 0.1$

The results and statistical analysis of the qualitative RT-PCR assay for glyceraldehyde-3-phosphate-dehydrogenase (gapdh) and lytic (orf29) or latent (orf73) mRNA for two independent experiments of implants infected with KSHV derived from BCBL-1 cells or UV-inactivated virus. Shown is the number of positive implants per total number of analyzed implants. *P* values were calculated using X^2 statistics.

In the SCID-hu Thy/Liv model, human B cells do not migrate outside the implant. Consistent with this observation, no KSHV-specific signal could be detected in the spleens of infected animals (data not shown), suggesting that the infection was species specific and did not spread to murine tissue.

Ganciclovir Interferes with Establishment and Maintenance of Infection. As ganciclovir inhibits KSHV replication in vitro (48, 49), we investigated whether the drug would also inhibit KSHV infection in the SCID-hu Thy/Liv model. Six infected animals were treated with twice-daily intraperitoneal injection of 50 mg/kg/d ganciclovir beginning at the time of KSHV inoculation. To concentrate our analysis specifically on productively infected cells, we quantitatively analyzed spliced transcript levels rather than viral DNA.

ABI Taqman® technology was used for real-time quantitative RT-PCR analysis (43). RNA was prepared and amplified in duplicate using primers specific for either spliced lytic (primers tac29-5F, tac29-68R, and tac29-22T) or spliced latent messages (primer lat-273F or TAQ-F1 with lat-335R and lat-294T; Table I and Fig. 4). Primers for amplification of the lytic orf29 message were located on opposite sites of intron #1, and the fluorescently labeled oligonucleotide probe spanned the splice junction. Hence, only correctly spliced late messages for orf29 were detected (Fig. 4 B). For the amplification of latent messages, primers specific for the spliced orf72 message were used (Fig. 4 A). As these primers differed in sequence from those employed for qual-

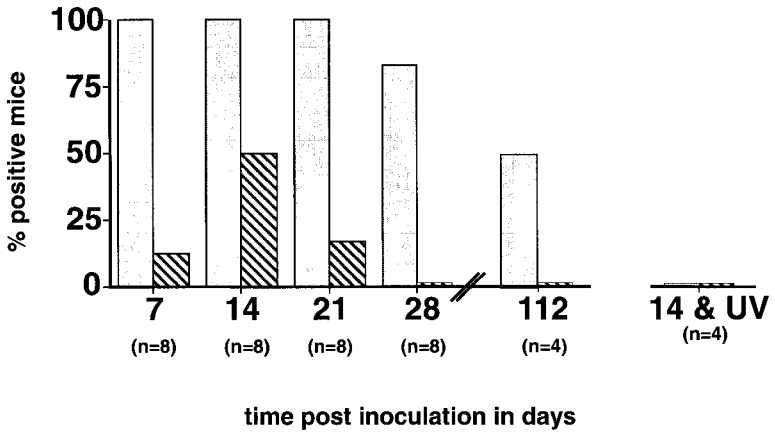

Figure 3. Time course of infection as determined by RT-PCR for the presence of latent (filled bars) or lytic (hatched bars) messages. Depicted is the percentage of implants giving a positive RT-PCR signal at indicated days after inoculation; n denotes the number of mice analyzed at each time point. The column with UV represents the signal obtained from implants that received UV-inactivated virus.

itative RT-PCR, RNA from each implant was analyzed twice for each transcript (qualitatively and quantitatively) using two different primer pairs. Implants that yielded significant signal using real-time quantitative RT-PCR always scored positive in the qualitative PCR, and samples that did not result in an amplified product using the qualitative RT-PCR and radioactive hybridization never showed a signal using real-time quantitative PCR and fluorescent detection. Only a single amplification product was produced in the quantitative RT-PCR reaction (data not shown). The amount of product was quantified at each cycle using a third specific, fluorescently labeled oligonucleotide present during the reaction. Hence, the number of cycles (ct) needed for the fluorescence intensity to reach a threshold value is a direct measure of the amount of amplified product. Based on control reactions using RNA from latently infected BCBL-1 cells, sensitivity limits were established to be 1–10 cells per reaction for the spliced latent orf72 assay and 100–1,000 cells per reaction for the lytic orf29 assays (Fig. 4, C and D), consistent with the observation that <3% of the population undergoes spontaneous lytic reactivation at any given time and the levels of orf29 mRNA in this population are much lower. The assay was linearly dependent on input RNA over three orders of magnitude.

Fig. 5 shows relative transcript levels in infected implants at day 14 after inoculation. Total RNA was isolated from individual implants in each group (implants injected with KSHV, implants injected with UV-inactivated KSHV, and implants injected with KSHV and treated with ganciclovir) and assayed in duplicate. To normalize for the amount of

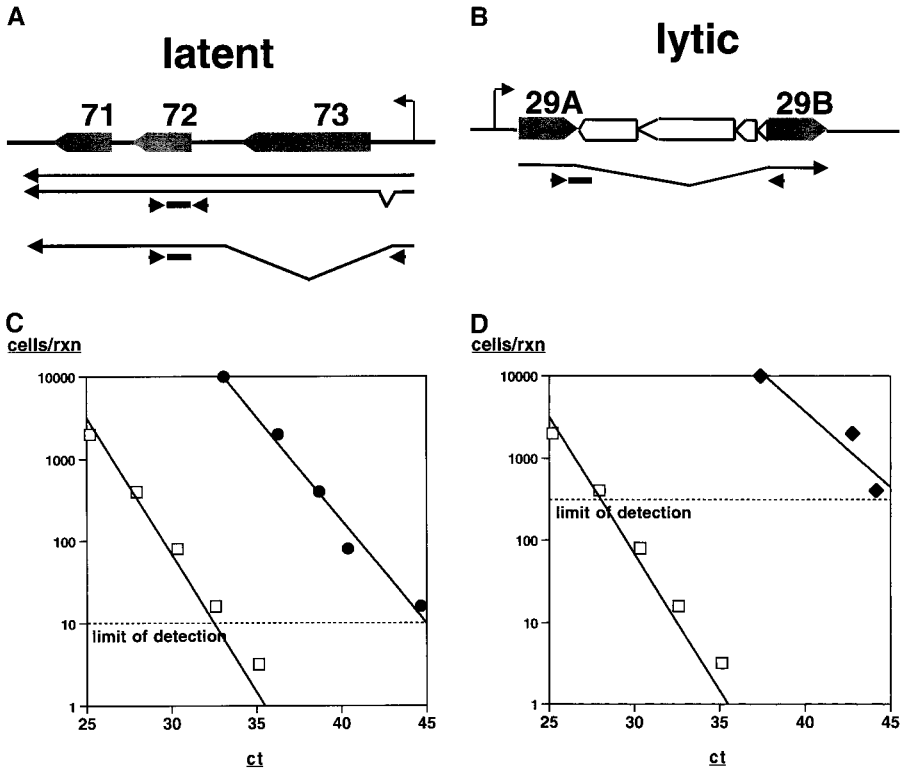

Figure 4. Primer design for quantitative RT-PCR. (A) The schematic outlines the genomic organization and message structure for orfs 71, 72, and 73 as determined previously (17). Arrows indicate given primers. (B) The schematic outlines the genomic organization and message structure of orf29 as determined previously (27). Arrows indicate given primers. C and D show detection levels for latent (C, ●) and lytic (D, ◆) probes compared with c-myc (□). The number of latent BCBL-1 cells per reaction is shown on the vertical axis, and the corresponding ct value as determined by real-time quantitative RT-PCR is shown on the horizontal axis.

RNA in each reaction, rRNA was coamplified and quantified using a differently labeled probe (primers riboF, riboR, and riboP; Table I). Ct values for KSHV-specific probes were subtracted from corresponding Ct values for rRNA and expressed as the number of latent or lytic cells per 10^6 cells (based on BCBL-1 control). As expected, implants injected with live virus exhibited significant levels of spliced latent ($P < 0.005$) and lytic ($P < 0.01$) transcripts compared with implants injected with UV-inactivated virus. Many animals displayed transcript levels that would correspond to 1 infected cell in 1,000 (assuming that transcript levels per cell are similar to those in BCBL-1 cells). Animals treated with ganciclovir showed a reduction in both latent ($P < 0.1$) and lytic ($P < 0.05$) transcript levels compared with untreated implants. RNA derived from latent BCBL-1 cells served as positive control. These data suggest that ganciclovir affected both the initial replication and subsequent spread of KSHV as well as establishment of latent infection, resulting in a decrease for both messages.

Productive KSHV Infection Occurs Predominantly in CD19$^+$ B Cells. To determine the cell tropism of KSHV in the Thy/Liv organ, we purified relevant cell populations from infected implants using flow cytometry and examined them for the presence of KSHV-specific transcripts (Fig. 6). B cells were identified by staining with anti-CD19–PE antibodies and T cells by staining with a mixture of FITC-coupled anti-CD4, anti-CD8, and anti-CD3 antibodies. As reported previously (31), an average of 0.5–2.5% of all cells in the implant were committed to the B cell lineage, as indicated by CD19 expression, whereas >90% of the implant cells were thymocytes, as indicated by CD3 expression (Fig. 6 A, implant). A fraction of the implant was used to isolate 10^6 CD3$^+$ thymocytes directly using flow cytometry. The remainder of the implant was depleted of thymocytes using biotinylated anti-CD3 and anti-CD8 antibodies coupled to

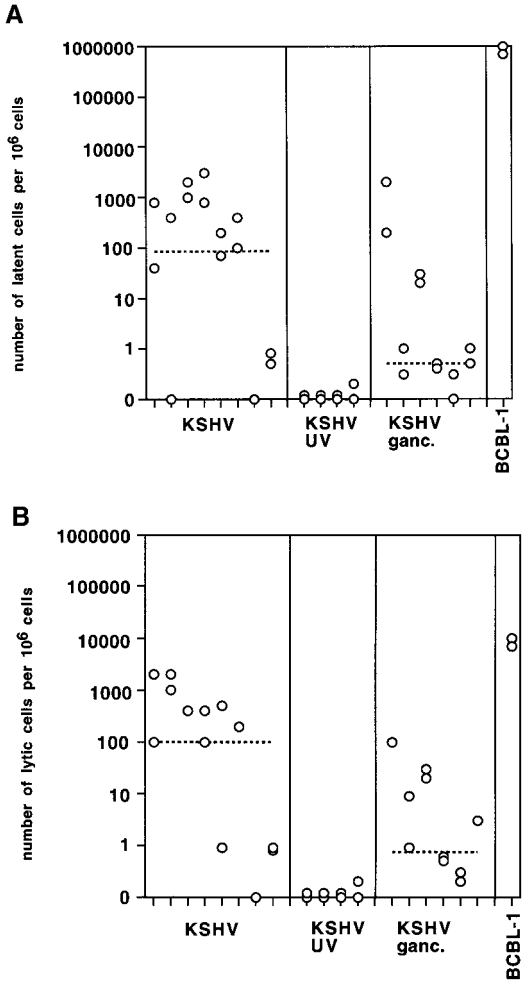

Figure 5. Analysis of transcript levels in infected implants. A and B show latent and lytic transcript levels expressed as the number of latent or lytic cells per 10^6 cells (logarithmic scale) for implants at day 14 after inoculation that were infected with KSHV (KSHV), infected with KSHV and treated with ganciclovir (KSHV ganc.), or infected with UV-inactivated virus (KSHV UV); BCBL-1 cells are shown as control. The median of each group is indicated by the dashed line. *P* values were calculated using the nonparametric Mann-Whitney test.

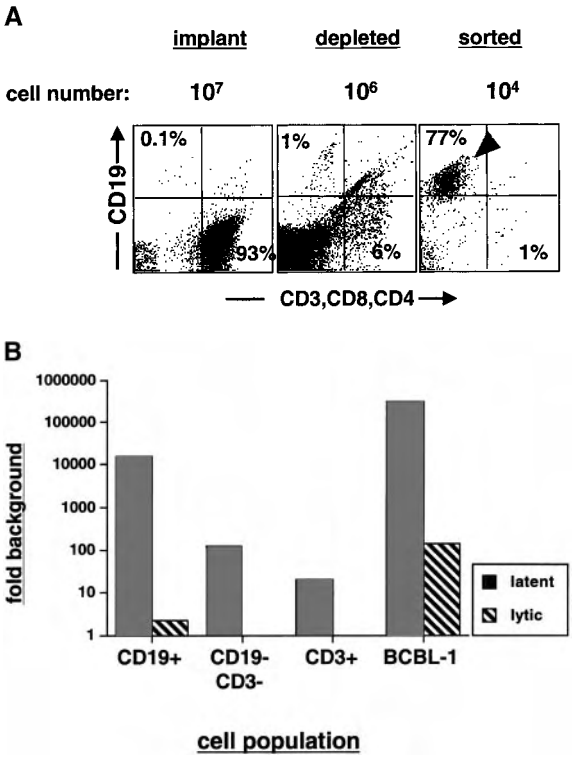

Figure 6. Tissue tropism of KSHV in infected SCID-hu Thy/Liv mice. (A) Representative FACScan™ analysis for CD19 (vertical) or combined CD4$^+$, CD8$^+$, and CD3$^+$ (horizontal) in cells pooled from three KSHV-infected implants harvested 14 d after inoculation: before T cell depletion (implant), after T cell depletion (depleted), or after sorting for CD19$^+$ cells of the depleted cell population (sorted). The total number of cells in the sample is also indicated. The percentage of CD19–PE or CD4–, CD8–, CD3–FITC$^+$ cells is shown in the upper left and lower right quadrants, respectively. B shows the levels of KSHV-specific latent/orf73 (filled bar) or lytic (hatched bar) transcripts in the indicated cell populations. All samples were assayed in duplicate and normalized for rRNA content. Standard deviations were too small to be visible on this scale. Levels are expressed as fold background (logarithmic scale) from uninfected CD19 cells.

streptavidin-linked magnetic beads (Fig. 6 A, depleted). The depleted population was stained with CD19–PE and avidin–FITC, and CD19 single-positive cells were isolated by flow cytometry. Although only 40,000 $CD19^+$ cells could be obtained for analysis, KSHV-specific latent and lytic transcripts could be detected in this cell population. This is consistent with previous observations, which detected KSHV in peripheral blood $CD19^+$ B cells (27, 47, 50). Low levels of KSHV-specific latent but never lytic transcripts were also detected in the cells negative for CD3, CD4, CD8, and CD19. We would expect to find stromal cells and macrophages in this population, which harbors KSHV in KS tumors (51). Experiments to determine the exact nature of these cells as well as the level of KSHV gene expression in them are currently underway. Even lower levels of latent transcript were detected in cells positive for CD3, i.e., T cells. Although we cannot exclude the possibility that the signal originates from contaminating B cells, reanalysis of the sorted CD3, CD4, and CD8 fractions determined them to be $\geq$99% $CD3^+$ (data not shown).

Histological (hematoxylin and eosin stain) and flow cytometric analysis (using mAbs directed against CD19, CD20, and CD45) showed no evidence of B cell depletion during the first 4 wk of infection. During this time frame, in fact, KSHV infection of the Thy/Liv implant was not correlated with any histopathologic changes (data not shown). We are currently following a cohort of infected mice to assess long-term consequences of infection.

Coinfection of SCID-hu Thy/Liv Mice with HIV-1 and KSHV. To test whether an interaction between KSHV and HIV-1 might occur in coinfected implants, cohorts of SCID-hu Thy/Liv mice were injected with a mixture of HIV-1 and KSHV or with each virus alone. The pathogenic, syncytium-inducing HIV-1 isolate NL4-3 was used at an input inoculum of 10^3 tissue culture $(TC)ID_{50}$. This strain induces massive T cell depletion starting at day 14 after inoculation, with <85% of implant thymocytes being destroyed by day 28–35 (42). Accordingly, we chose to examine the coinfected implants on day 14, when HIV-1 infection is well established but before the onset of T cell death complicates the analysis of effects on viral load. KSHV viral load and HIV-1 p24 and RNA levels were quantitated at this time point (Fig. 7). Relative to animals infected with KSHV alone, no difference was noted in the levels of KSHV DNA in animals coinfected with HIV-1 and KSHV. The mean KSHV-specific DNA PCR signal in these two cohorts

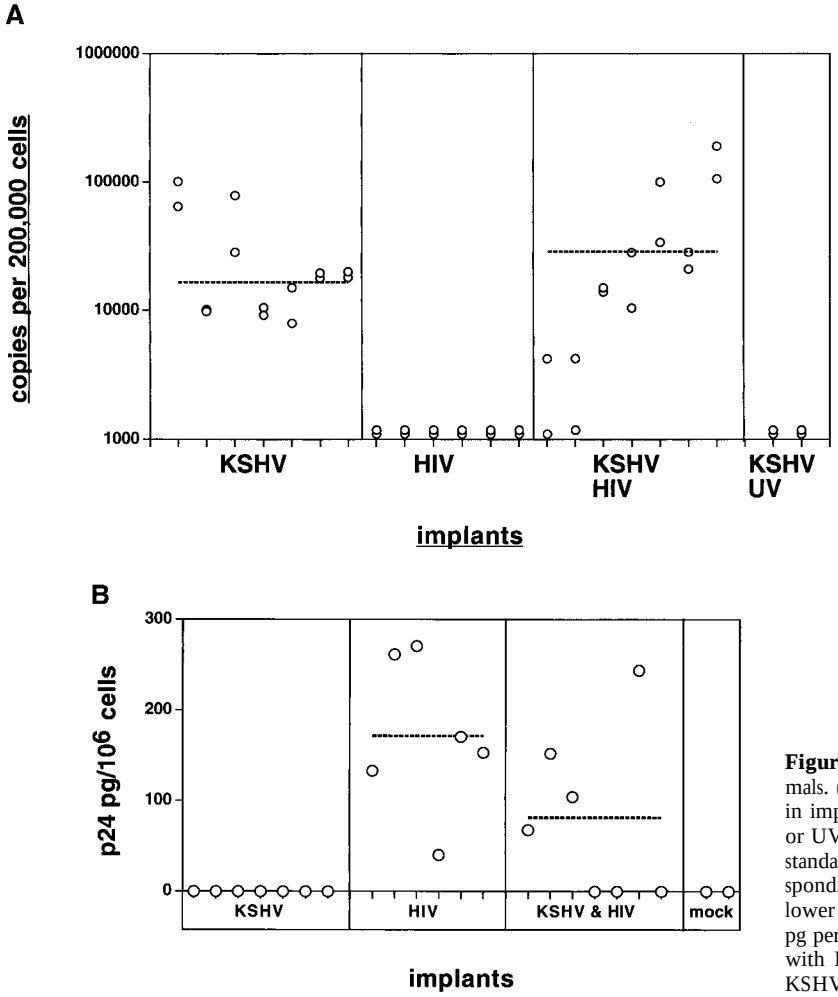

Figure 7. HIV-1 and KSHV viral load in coinfected animals. (A) KSHV genome copy number (○) per 200,000 cells in implants infected with KSHV, HIV-1, HIV-1, and KSHV or UV-inactivated KSHV and HIV-1. The right side depicts a standard curve for dilution series of pDD4 and the corresponding fluorescent threshold (ct). Dashed line indicates the lower limit of detection in this assay. (B) HIV-1 p24 levels in pg per 10^6 cells (○) in implants 14 d after inoculation infected with KSHV, HIV-1, HIV-1, and KSHV or UV-inactivated KSHV and HIV-1 (mock).

was 10–100 times the signal obtained from animals infected with UV-inactivated virus or HIV-1 alone, suggesting that KSHV replicated as in previous experiments and that its level of replication was unaffected by HIV-1. Correspondingly, the level of HIV-1 p24 in the implant was reduced only minimally in animals coinfected with KSHV as compared with animals infected with HIV-1 alone. We conclude that KSHV did not significantly influence HIV-1 replication, at least in the short period of acute coinfection.

Discussion

The absence of an appropriate animal model to study de novo infection has severely limited our understanding of the biology of KSHV. This paper reports the first small animal model for de novo infection by KSHV. It demonstrates that BCBL-1–derived KSHV preparations can infect SCID-hu Thy/Liv mice, resulting in transient lytic replication and persistent latent infection, as judged by (a) the increase in genome copy number and (b) the presence of latent and lytic viral transcripts in infected animals.

Flow cytometric analysis demonstrates that KSHV replicates primarily in $CD19^+$ B cell populations of the implant, which is consistent with the tropism described for KSHV in humans (47, 51–53). As KSHV does not replicate in SCID mice (30) that have received human peripheral blood leukocytes (a model that does not support hematopoiesis; reference 29), our observations suggest that immature or developing cell populations may serve as the predominant target of KSHV infection. Alternatively, it is possible that transmission to human blood cells requires a lymphoid microenvironment not reproduced by the implant. Dissecting the tissue tropism of KSHV in detail and mapping KSHV gene expression in different host cells will be one of the major uses of the SCID-hu Thy/Liv system.

The presence of lytic replication during the early phase of infection suggests another potential application of this model: to assess the impact of antivirals and biological response modifiers on KSHV replication in vivo, similar to its established use in the development of anti-HIV drugs. The susceptibility of KSHV infection to ganciclovir in vivo faithfully mirrors prior in vitro findings and affirms that this model, once optimized, may become a useful part of preclinical drug development.

Coinfection with HIV-1 did not enhance or interfere with KSHV replication, and the presence of KSHV did not influence the replication kinetics or cytopathogenicity induced by HIV-1. KSHV encodes viral chemokines that block interactions between HIV-1 and CCR5/CCR3 in vitro (54–56), raising the speculation that this mechanism might also be operational in vivo (for review see reference 57). The absence of a significant effect of KSHV on HIV-1 replication argues against this, although the small number of KSHV-infected cells in the implant does not allow us to entirely exclude the possibility of interactions in vivo. HIV-1 itself is known to induce a number of cytokines (IFN-γ, TNF-α, IL-1, and IL-6), and these as well as HIV-1 Tat itself have been proposed to be involved in the development of KS (for review see reference 58). Although analogous changes in cytokine expression may occur in HIV-1–infected SCID-hu Thy/Liv implants compared with infected PBMCs, no effect of HIV-1 on KSHV replication was observed, suggesting that HIV-1–induced cofactors did not have an impact on KSHV replication in this context. Ongoing experiments are now testing the possibility that interactions between HIV-1 and KSHV might be observed after coinfection with different isolates of HIV-1 and/or after longer periods of time.

KSHV infection of the Thy/Liv implant did not produce detectable histological phenotypes reminiscent of known KSHV-related human diseases. Certainly the model was not expected to reproduce KS, a neoplasm involving poorly understood cells of endothelial lineage (5). Although some $CD34^+$ cells are doubtless present in the implant, it is unlikely that the full range of endothelial precursors, stromal components, and growth factors needed to support KS development would be present in this system. Rather, the model was designed to examine infection of the lymphoid compartment. The model successfully produces transient lytic infection and more sustained viral persistence and appears to mirror the correct tissue tropism of infection. However, it did not give evidence for lymphoid depletion or lymphoproliferation. Although the small number of B cells present in the implant severely constrained our ability to score for B cell depletion, the proportion of $CD19^+$ cells did not appear to diminish over time. Similarly, we did not observe expansion of the B cell population and did not detect features reminiscent of Castleman's disease or PEL. However, it is important to remember that both of these phenotypes are exceedingly rare manifestations of human KSHV infection. Judging from the fact that $\sim$5–7% of healthy subjects are KSHV seropositive, it is likely that most primary infections with this agent are subclinical or asymptomatic. Thus, it is not clear that the relatively bland histologic picture generated here is not representative of many human primary infections. We are continuing to study the model to see if disease appears at late times after inoculation or if the system can be experimentally modified to allow induction of cell injury or proliferation. In the meantime, in addition to its potential uses in drug screening, the model offers an excellent opportunity to better define in detail which subsets of $CD19^+$ cells are most permissive for KSHV and whether and how efficiently T cells and macrophages can be targets of infection.

We thank Eric Wieder and Lisa Gibson for expert flow cytometry.

Kinetic PCR analysis was supported by Robert M. Grant and Jerry Kropp of the Gladstone/UCSF Laboratory of Clinical Virology (#P30 MH59037; University of California at San Francisco/Macy's Center for

Creative Therapies). This work was supported by the Howard Hughes Medical Institute and Public Health Service grants to D. Ganem and National Institutes of Health grants AI-65309 and AI-40312 to J.M. McCune. J.M. McCune is an Elisabeth Glaser Scientist supported by the Elizabeth Glaser Pediatric AIDS Foundation. R. Renne is a Fellow of the Leukemia Society.

Address correspondence to Donald Ganem, Dept. of Microbiology and Immunology, University of California, 513 Parnassus Ave., HSE403, San Francisco, CA 94143-0414. Phone: 415-476-2826; Fax: 415-476-0939; E-mail: ganem@socrates.ucsf.edu

Submitted: 19 May 1999 Revised: 21 August 1999 Accepted: 28 September 1999

References

1. Chang, Y., E. Cesarman, M.S. Pessin, F. Lee, J. Culpepper, D.M. Knowles, and P.S. Moore. 1994. Identification of herpesvirus-like DNA sequences in AIDS-associated Kaposi's sarcoma. *Science*. 266:1865–1869.
2. Cesarman, E., Y. Chang, P.S. Moore, J.W. Said, and D.M. Knowles. 1995. Kaposi's sarcoma-associated herpesvirus-like DNA sequences in AIDS-related body-cavity-based lymphomas. *N. Engl. J. Med.* 332:1186–1191.
3. Soulier, J., L. Grollet, E. Oksenhendler, P. Cacoub, D. Cazals-Hatem, P. Babinet, M.F. d'Agay, J.P. Clauvel, M. Raphael, L. Degos, et al. 1995. Kaposi's sarcoma-associated herpesvirus-like DNA sequences in multicentric Castleman's disease. *Blood*. 86:1276–1280.
4. Ganem, D. 1997. KSHV and Kaposi's sarcoma: the end of the beginning? *Cell*. 91:157–160.
5. Boshoff, C., and R.A. Weiss. 1997. Aetiology of Kaposi's sarcoma: current understanding and implications for therapy. *Mol. Med. Today*. 3:488–494.
6. Schulz, T.F. 1998. Kaposi's sarcoma-associated herpesvirus (human herpesvirus-8). *J. Gen. Virol*. 79:1573–1591.
7. Moore, P.S., and Y. Chang. 1998. Kaposi's sarcoma-associated herpesvirus-encoded oncogenes and oncogenesis. *J. Natl. Cancer Inst. Monogr*. 23:65–71.
8. Moore, P.S., and Y. Chang. 1995. Detection of herpesvirus-like DNA sequences in Kaposi's sarcoma in patients with and without HIV infection. *N. Engl. J. Med*. 332:1181–1185.
9. Miller, G., M.O. Rigsby, L. Heston, E. Grogan, R. Sun, C. Metroka, J.A. Levy, S.J. Gao, Y. Chang, and P. Moore. 1996. Antibodies to butyrate-inducible antigens of Kaposi's sarcoma-associated herpesvirus in patients with HIV-1 infection. *N. Engl. J. Med*. 334:1292–1297.
10. Kedes, D.H., D. Ganem, N. Ameli, P. Bacchetti, and R. Greenblatt. 1997. The prevalence of serum antibody to human herpesvirus 8 (Kaposi sarcoma-associated herpesvirus) among HIV-seropositive and high-risk HIV-seronegative women. *JAMA (J. Am. Med. Assoc.)* 277:478–481.
11. Gao, S.J., L. Kingsley, D.R. Hoover, T.J. Spira, C.R. Rinaldo, A. Saah, J. Phair, R. Detels, P. Parry, Y. Chang, et al. 1996. Seroconversion to antibodies against Kaposi's sarcoma-associated herpesvirus-related latent nuclear antigens before the development of Kaposi's sarcoma. *N. Engl. J. Med*. 335: 233–241.
12. Kedes, D.H., E. Operskalski, M. Busch, R. Kohn, J. Flood, and D. Ganem. 1996. The seroepidemiology of human herpesvirus 8 (Kaposi's sarcoma-associated herpesvirus): distribution of infection in KS risk groups and evidence for sexual transmission. *Nat. Med*. 2:918–924.
13. Martin, J.N., D.E. Ganem, D.H. Osmond, K.A. Page-Shafer, D. Macrae, and D.H. Kedes. 1998. Sexual transmission and the natural history of human herpesvirus 8 infection. *N. Engl. J. Med*. 338:948–954.
14. Whitby, D., M.R. Howard, M. Tenant-Flowers, N.S. Brink, A. Copas, C. Boshoff, T. Hatzioannou, F.E. Suggett, D.M. Aldam, A.S. Denton, et al. 1995. Detection of Kaposi sarcoma associated herpesvirus in peripheral blood of HIV-infected individuals and progression to Kaposi's sarcoma. *Lancet*. 346:799–802.
15. Zhong, W., H. Wang, B. Herndier, and D. Ganem. 1996. Restricted expression of Kaposi sarcoma-associated herpesvirus (human herpesvirus 8) genes in Kaposi sarcoma. *Proc. Natl. Acad. Sci. USA*. 93:6641–6646.
16. Staskus, K.A., W. Zhong, K. Gebhard, B. Herndier, H. Wang, R. Renne, J. Beneke, J. Pudney, D.J. Anderson, D. Ganem, et al. 1997. Kaposi's sarcoma-associated herpesvirus gene expression in endothelial (spindle) tumor cells. *J. Virol*. 71:715–719.
17. Dittmer, D., M. Lagunoff, R. Renne, K. Staskus, A. Haase, and D. Ganem. 1998. A cluster of latently expressed genes in Kaposi's sarcoma-associated herpesvirus. *J. Virol*. 72:8309–8315.
18. Davis, M.A., M.A. Sturzl, C. Blasig, A. Schreier, H.G. Guo, M. Reitz, S.R. Opalenik, and P.J. Browning. 1997. Expression of human herpesvirus 8-encoded cyclin D in Kaposi's sarcoma spindle cells. *J. Natl. Cancer Inst*. 89:1868–1874.
19. Sturzl, M., C. Blasig, A. Schreier, F. Neipel, C. Hohenadl, E. Cornali, G. Ascherl, S. Esser, N.H. Brockmeyer, M. Ekman, et al. 1997. Expression of HHV-8 latency-associated T0.7 RNA in spindle cells and endothelial cells of AIDS-associated, classical and African Kaposi's sarcoma. *Int. J. Cancer*. 72:68–71.
20. Muralidhar, S., A.M. Pumfery, M. Hassani, M.R. Sadaie, N. Azumi, M. Kishishita, J.N. Brady, J. Doniger, P. Medveczky, and L.J. Rosenthal. 1998. Identification of kaposin (open reading frame K12) as a human herpesvirus 8 (Kaposi's sarcoma-associated herpesvirus) transforming gene. *J. Virol*. 72: 4980–4988.
21. Swanton, C., D.J. Mann, B. Fleckenstein, F. Neipel, G. Peters, and N. Jones. 1997. Herpes viral cyclin/Cdk6 complexes evade inhibition by CDK inhibitor proteins. *Nature*. 390:184–187.
22. Renne, R., W. Zhong, B. Herndier, M. McGrath, N. Abbey, D. Kedes, and D. Ganem. 1996. Lytic growth of Kaposi's sarcoma-associated herpesvirus (human herpesvirus 8) in culture. *Nat. Med*. 2:342–346.
23. Kirshner, J.R., K. Staskus, A. Haase, M. Lagunoff, and D. Ganem. 1999. Expression of the open reading frame 74 (G-protein-coupled receptor) gene of Kaposi's sarcoma (KS)-

associated herpesvirus: implications for KS pathogenesis. *J. Virol*. 73:6006–6014.
24. Gao, S.J., C. Boshoff, S. Jayachandra, R.A. Weiss, Y. Chang, and P.S. Moore. 1997. KSHV ORF K9 (vIRF) is an oncogene which inhibits the interferon signaling pathway. *Oncogene*. 15:1979–1985.
25. Bais, C., B. Santomasso, O. Coso, L. Arvanitakis, E.G. Raaka, J.S. Gutkind, A.S. Asch, E. Cesarman, M.C. Gershengorn, E.A. Mesri, et al. 1998. G-protein-coupled receptor of Kaposi's sarcoma-associated herpesvirus is a viral oncogene and angiogenesis activator. *Nature*. 391:86–89.
26. Lee, H., R. Veazey, K. Williams, M. Li, J. Guo, F. Neipel, B. Fleckenstein, A. Lackner, R.C. Desrosiers, and J.U. Jung. 1998. Deregulation of cell growth by the K1 gene of Kaposi's sarcoma-associated herpesvirus. *Nat. Med*. 4:435–440.
27. Renne, R., D. Blackbourn, D. Whitby, J. Levy, and D. Ganem. 1998. Limited transmission of Kaposi's sarcoma-associated herpesvirus in cultured cells. *J. Virol*. 72:5182–5188.
28. Foreman, K.E., J. Friborg, Jr., W.P. Kong, C. Woffendin, P.J. Polverini, B.J. Nickoloff, and G.J. Nabel. 1997. Propagation of a human herpesvirus from AIDS-associated Kaposi's sarcoma. *N. Engl. J. Med*. 336:163–171.
29. Mosier, D.E., R.J. Gulizia, S.M. Baird, and D.B. Wilson. 1988. Transfer of a functional human immune system to mice with severe combined immunodeficiency. *Nature*. 335: 256–259.
30. Picchio, G.R., R.E. Sabbe, R.J. Gulizia, M. McGrath, B.G. Herndier, and D.E. Mosier. 1997. The KSHV/HHV8-infected BCBL-1 lymphoma line causes tumors in SCID mice but fails to transmit virus to a human peripheral blood mononuclear cell graft. *Virology*. 238:22–29.
31. Namikawa, R., K.N. Weilbaecher, H. Kaneshima, E.J. Yee, and J.M. McCune. 1990. Long-term human hematopoiesis in the SCID-hu mouse. *J. Exp. Med*. 172:1055–1063.
32. McCune, J.M., R. Namikawa, H. Kaneshima, L.D. Shultz, M. Lieberman, and I.L. Weissman. 1988. The SCID-hu mouse: murine model for the analysis of human hematolymphoid differentiation and function. *Science*. 241:1632–1639.
33. Namikawa, R., H. Kaneshima, M. Lieberman, I.L. Weissman, and J.M. McCune. 1988. Infection of the SCID-hu mouse by HIV-1. *Science*. 242:1684–1686.
34. Feuer, G., J.K. Fraser, J.A. Zack, F. Lee, R. Feuer, and I.S. Chen. 1996. Human T-cell leukemia virus infection of human hematopoietic progenitor cells: maintenance of virus infection during differentiation in vitro and in vivo. *J. Virol*. 70: 4038–4044.
35. Gobbi, A., C.A. Stoddart, M.S. Malnati, G. Locatelli, F. Santoro, N.W. Abbaey, C. Bare, V. Linquist-Stepps, M.E. Moreno, B.G. Herndier, et al. 1999. Human herpesvirus 6 (HHV-6) causes severe thymocyte depletion in SCID-hu Thy/Liv Mice. *J. Exp. Med*. 189:1953–1960.
36. Moffat, J.F., M.D. Stein, H. Kaneshima, and A.M. Arvin. 1995. Tropism of varicella-zoster virus for human $CD4^+$ and $CD8^+$ T lymphocytes and epidermal cells in SCID-hu mice. *J. Virol*. 69:5236–5242.
37. Berkowitz, R.D., S. Alexander, C. Bare, V. Linquist-Stepps, M. Bogan, M.E. Moreno, L. Gibson, E.D. Wieder, J. Kosek, C.A. Stoddart, et al. 1998. CCR5- and CXCR4-utilizing strains of human immunodeficiency virus type 1 exhibit differential tropism and pathogenesis in vivo. *J. Virol*. 72:10108–10117.
38. Mocarski, E.S., M. Bonyhadi, S. Salimi, J.M. McCune, and H. Kaneshima. 1993. Human cytomegalovirus in a SCID-hu mouse: thymic epithelial cells are prominent targets of viral replication. *Proc. Natl. Acad. Sci. USA*. 90:104–108.
39. Auwaerter, P.G., H. Kaneshima, J.M. McCune, G. Wiegand, and D.E. Griffin. 1996. Measles virus infection of thymic epithelium in the SCID-hu mouse leads to thymocyte apoptosis. *J. Virol*. 70:3734–3740.
40. Bonyhadi, M.L., L. Rabin, S. Salimi, D.A. Brown, J. Kosek, J.M. McCune, and H. Kaneshima. 1993. HIV induces thymus depletion in vivo. *Nature*. 363:728–732.
41. Stoddart, C.A., L. Rabin, M. Hincenbergs, M. Moreno, V. Linquist-Stepps, J.M. Leeds, L.A. Truong, J.R. Wyatt, D.J. Ecker, and J.M. McCune. 1998. Inhibition of human immunodeficiency virus type 1 infection in SCID-hu Thy/Liv mice by the G-quartet-forming oligonucleotide, ISIS 5320. *Antimicrob. Agents Chemother*. 42:2113–2115.
42. Rabin, L., M. Hincenbergs, M.B. Moreno, S. Warren, V. Linquist, R. Datema, B. Charpiot, J. Seifert, H. Kaneshima, and J.M. McCune. 1996. Use of standardized SCID-hu Thy/Liv mouse model for preclinical efficacy testing of anti-human immunodeficiency virus type 1 compounds. *Antimicrob. Agents Chemother*. 40:755–762.
43. Heid, C.A., J. Stevens, K.J. Livak, and P.M. Williams. 1996. Real time quantitative PCR. *Genome Res*. 6:986–994.
44. Longo, M.C., M.S. Berninger, and J.L. Hartley. 1990. Use of uracil DNA glycosylase to control carry-over contamination in polymerase chain reactions. *Gene*. 93:125–128.
45. van der Eb, A.J., and J.A. Cohen. 1967. The effect of UV-irradiation on the plaque-forming ability of single- and double-stranded polyoma virus DNA. *Biochem. Biophys. Res. Commun*. 28:284–288.
46. Latarjet, R., R. Cramer, and L. Montagnier. 1967. Inactivation, by UV-, x-, and gamma-radiations, of the infecting and transforming capacities of polyoma virus. *Virology*. 33:104–111.
47. Mesri, E.A., E. Cesarman, L. Arvanitakis, S. Rafii, M.A. Moore, D.N. Posnett, D.M. Knowles, and A.S. Asch. 1996. Human herpesvirus-8/Kaposi's sarcoma–associated herpesvirus is a new transmissible virus that infects B cells. *J. Exp. Med*. 183:2385–2390.
48. Kedes, D.H., and D. Ganem. 1997. Sensitivity of Kaposi's sarcoma-associated herpesvirus replication to antiviral drugs. Implications for potential therapy. *J. Clin. Invest*. 99:2082–2086.
49. Medveczky, M.M., E. Horvath, T. Lund, and P.G. Medveczky. 1997. In vitro antiviral drug sensitivity of the Kaposi's sarcoma-associated herpesvirus. *AIDS*. 11:1327–1332.
50. Blackbourn, D.J., J. Ambroziak, E. Lennette, M. Adams, B. Ramachandran, and J.A. Levy. 1997. Infectious human herpesvirus 8 in a healthy North American blood donor. *Lancet*. 349:609–611.
51. Blasig, C., C. Zietz, B. Haar, F. Neipel, S. Esser, N.H. Brockmeyer, E. Tschachler, S. Colombini, B. Ensoli, and M. Sturzl. 1997. Monocytes in Kaposi's sarcoma lesions are productively infected by human herpesvirus 8. *J. Virol*. 71:7963–7968.
52. Kliche, S., E. Kremmer, W. Hammerschmidt, U. Koszinowski, and J. Haas. 1998. Persistent infection of Epstein-Barr virus-positive B lymphocytes by human herpesvirus 8. *J. Virol*. 72:8143–8149.
53. Decker, L.L., P. Shankar, G. Khan, R.B. Freeman, B.J. Dezube, J. Lieberman, and D.A. Thorley-Lawson. 1996. The Kaposi sarcoma–associated herpesvirus (KSHV) is present as an intact latent genome in KS tissue but replicates in the peripheral blood mononuclear cells of KS patients. *J. Exp. Med*. 184:283–288.

54. Boshoff, C., Y. Endo, P.D. Collins, Y. Takeuchi, J.D. Reeves, V.L. Schweickart, M.A. Siani, T. Sasaki, T.J. Williams, P.W. Gray, et al. 1997. Angiogenic and HIV-inhibitory functions of KSHV-encoded chemokines. *Science*. 278: 290–294.
55. Kledal, T.N., M.M. Rosenkilde, F. Coulin, G. Simmons, A.H. Johnsen, S. Alouani, C.A. Power, H.R. Luttichau, J. Gerstoft, P.R. Clapham, et al. 1997. A broad-spectrum chemokine antagonist encoded by Kaposi's sarcoma-associated herpesvirus. *Science*. 277:1656–1659.
56. Moore, P.S., C. Boshoff, R.A. Weiss, and Y. Chang. 1996. Molecular mimicry of human cytokine and cytokine response pathway genes by KSHV. *Science*. 274:1739–1744.
57. Dittmer, D., and D.H. Kedes. 1998. Do viral chemokines modulate Kaposi's sarcoma? *Bioessays*. 20:367–370.
58. Gallo, R.C. 1998. The enigmas of Kaposi's sarcoma. *Science*. 282:1837–1839.